ChemComm

Accepted Manuscript

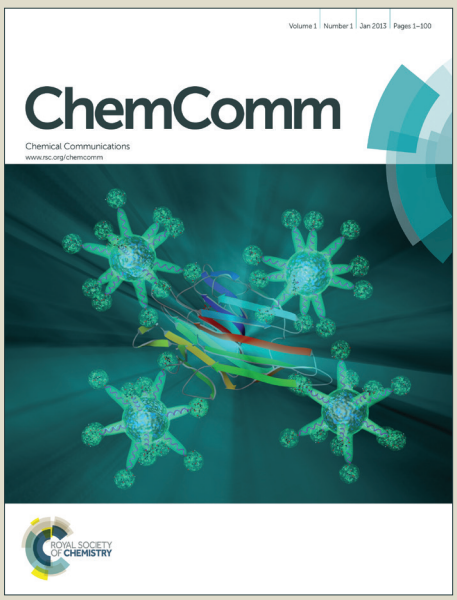

ROYAL SOCIETY OF CHEMISTRY

www.rsc.org/chemcomm

TOC:
L-chain apoferritin can be turned into a more stable and cellular active ferroxidase with nanoparticles as the artificial active sites.

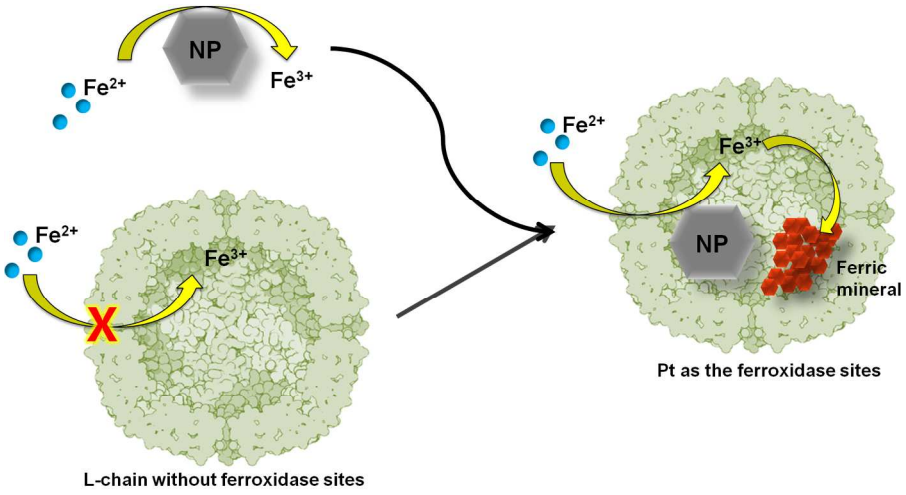

Journal Name

RSCPublishing

COMMUNICATION

Semi-Artificial and Bioactive Ferroxidase with a Nanoparticle as the Active Site

Cite this: DOI: 10.1039/x0xx00000x

L. Li,[a] L. Zhang,*[a] U. Carmona[a] and M. Knez*[a,b]

Received 00th January 2012,
Accepted 00th January 2012

DOI: 10.1039/x0xx00000x

www.rsc.org/

Light-chain apoferritin is lacking ferroxidase activity, which can be supplemented with Pt-nanoparticles. The hybrid bioinorganic nanoparticle outperforms its heavy-chain pendant in terms of ferroxidase activity, mineralization ability and inhibition resistance. Being active in a cellular environment it regulates the iron homeostasis.

Enzymes catalyze reactions of biological processes in a specific and efficient way. However, most enzymes, especially their catalytic active sites, are very sensitive to alterations of the microenvironment including, temperature, pH or ions. Modern computational design and biotechnological engineering pathways still rely on amino acids as constituting parts only, restricting the stability of the enzymes by the inherent instability of their natural building blocks.[1] Recently, catalytically active nanoparticles (NPs) have show their potential as biomimetic enzymes.[2] The advantage of the approach is that inorganic nanoparticles accept a much larger bandwidth of environmental conditions without loss of functionality. Here we present a novel approach towards engineering stable and bioactive enzymes by incorporating nanoparticles as enzyme active sites into a protein scaffold.

Ferroxidases are important for the cellular transport and the storage of iron, an essential metal for biological enzymes, the O_2 transport, immune defense, the energy metabolism, etc. Impaired ferroxidase activity is found to contribute to the generation or progress of diseases.[3] For example, the ferroxidase activity of ceruloplasmin is oxidatively inhibited by Parkinson's disease.[4] The ferroxidase activity of β-amyloid protein precursor (APP) is specifically inhibited by Zn^{2+} in Alzheimer's disease.[5] Besides APP, Zn^{2+} also inhibits the ferroxidase activity of heavy chain (21kDa) composed ferritin. Ferritin is a hollow protein complex of 24 subunits (apoferritin) containing a ferrihydrite core. The subunit can be light (L)- or heavy (H)-chain polypeptides. The L-chain (19kDa) has no ferroxidase activity. However, a more efficient mineralization of ferric ions inside the cavity occurs in the presence of L-chains.[6] Based on this fact, it is rational that a stable ferroxidase with efficient iron mineralization ability can be assembled from an inorganic ferroxidase and L-chain proteins The nanoparticle of the engineered hybrid enzyme oxidizes ferrous ion to ferric ion, while the protein part mineralizes the ferric ion, which would otherwise precipitate in an aqueous enviroment.

With the intention to use a NP as the ferroxidase active site, we followed well-established methods for synthesizing metal NPs within the cavities of human L-chain (apo-huFL) and H-chain (apo-huFH) apoferritins. Such compositions, especially with gold or platinum NPs, are well-known to exhibit oxidase activities.[7-8] UV-vis spectroscopy was performed in order to determine the kinetics of the catalytic reactions of the components for iron oxidation in aerobic conditions. An absorbance around 300 nm is characteristic for ferroxidase catalyzed iron oxidation.[9] Rapid oxidation of iron within seconds was observed with apo-huFH, which exhibits natural ferroxidase activity (Fig. 1A). As expected, apo-huFL was ferroxidase inactive and the spectra at 250-300 nm showed only non-enzymatic iron oxidation. However, enzymatic iron oxidation was observed with platinum nanoparticles inside the cavity of L-chain apoferritin (Pt-huFL). The stepwise progressing iron oxidation with Pt-huFL indicates that the mechanism of the nanoparticle surface-catalyzed ferroxidation is different to that of amino acid residues-catalyzed reaction by apo-huFH, presumably related to fundamentally differing binding, conversion and dissociation chemistry of substrates and products. Despite a slower catalytic rate of Pt-huFL, a similar total iron oxidation rate was achieved with both Pt-huFL and apo-huFH. Note that the ferroxidase activity of the nanoparticles is material specific: Encapsulated gold nanoparticles (Au-huFL) did not exhibit ferroxidase activity (Fig.1A).

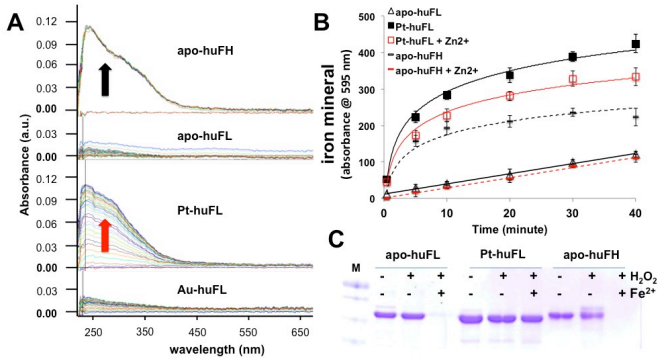

Fig. 1 (A) Ferroxidase activity kinetically measured within 2 min with UV-vis spectroscopy. The reaction was performed with 1 µM protein, 40 µM Fe^{2+} and 50 mM Tris at pH 7.0. (B) Fe^{3+} evolution over time determined with the XO assay. The assay was performed with 0.2 µM protein, 10 µM Fe^{2+} and 50 mM Tris at pH 7.0. The inhibition of ferroxidase activity was performed in the presence of 10 mM Zn^{2+}. The results are presented by the mean ± SD. (C) SDS-PAGE of recombinant apo-huFL, apo-huFH and Pt-huFL after treatment with 50 mM H_2O_2 or/and 500 µM Fe^{2+} for 30 min. M: protein weight marker.

The Pt-huFL catalyzed ferroxidation was further confirmed by quantification of the ferric iron with xylenol orange (XO) which shows a high specificity for Fe^{3+} even in the presence of Zn^{2+} (Fig. S1). With the XO assay, not the initial rate of ferroxidation, but the formation of products (Fe^{3+}) is determined, which allows determination of the contribution of apo-huFL to the total reaction. With this experiment, again catalytic conversion to ferric ions was observed with apo-huFH and non-enzymatic formation with apo-huFL alone (Fig. 1B). However, with apo-huFH the evolution of ferric ions reached a quasi plateau after 10 min, while it was incessant with Pt-huFL during the whole assay period, resulting in a higher final ferric concentration (Fig. 1B). The incessant Fe^{3+} production with Pt-huFL indicates that the Pt nanoparticles altered the reaction mechanism and facilitated a more consistent ferroxidation than the natural ferroxidase apo-huFH (Fig. S2). In order to verify whether or not the oxidized iron was mineralized within the hybrid ferroxidase, the iron content of the purified ferritin after the catalytic reaction was determined. The combination of Pt-NP and L-type chains showed the most efficient iron mineralization with more than 2000 iron ions per apoferritin on the average (Fig. S3).

In agreement with already published data, the ferroxidase activity of apo-huFH showed strong inhibition with 10 mM Zn^{2+} (Fig. 1B). In the presence of Zn^{2+} the iron oxidation with apo-huFH turned non-enzymatic, similar to the case of ferroxidase inactive apo-huFL. An occupation of the active site of the enzyme by binding of Zn^{2+} to the catalytic residues may be the reason for the inhibition. This is rather unlikely to occur with nanoparticles as active sites. According to our assay, Zn^{2+} slightly lowers the ferroxidase activity of Pt-huFL by around 10%, but does not change the manner of the iron conversion course. A similar effect was observed with Pt-huFH (Fig. S4), which confirms that the different catalytic mechanism of Pt nanoparticles compared to enzymes induces Zn^{2+}-resistance. The small decrease of iron mineralization caused by Zn^{2+} may be due to the competitive transport of the two types of metal ions through the protein channel of apoferritin.

Besides the effects of Zn^{2+}, H_2O_2 was observed to evolve during the ferroxidation in mammalian apoferritins,[10] which can cause damage to ferritin in a deregulated cellular environment. Treatment with H_2O_2 alone did not affect the electrophoretic mobility and band intensity of the apoferritins and Pt-huFL (Fig. 1C). The observation that ferritin with a ferrihydrite core was degraded under the treatment indicates the key role of iron (Fig. S5). Indeed, apo-huFL or apo-huFH proteins completely degraded in simultaneous presence of both Fe^{2+} and H_2O_2 (Fig. 1C). Apparently, the ferrous iron stimulated the degradation of apoferritin, regardless of the ferroxidase activity. However, identical treatment of Pt-huFL did not result in protein degredation. The reason for this stabilization is that Pt-nanoparticles possess also catalase and superoxide dismutase (SOD) activity, which efficiently detoxify the harmful reactive oxygen species (ROS) produced during the iron metabolism.[8]

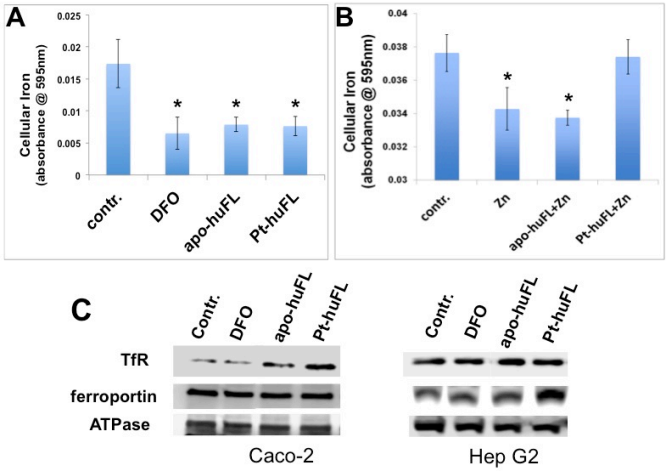

Fig. 2 Cellular iron content of Caco-2 cells after treatment with deferoxamine (DFO, 300 µM), apo- and Pt-huFL (50 µg/ml), (A) for 24 h. (B) in presence of 40 µM Zn^{2+}. Untreated cells were used as internal control (contr.). The values are presented by mean ± SD. *: $p < 0.001$. (C) Western analysis of the transferritin receptor (TfR) and ferroportin amounts in the cell membrane fractions upon the treatments. ATPase was detected as the loading control.

Under natural circumstances, the human body already utilizes endogenous ferritin both as an antioxidant and for iron depletion.[11] We expected that our bioinorganic ferroxidase nanozyme, especially the most active Pt-huFL, could actively influence the cellular iron level. Normally, the cells cannot distinguish apoferritin (iron free) from ferritin (iron containing), which opens the possibility to trick the cells in an "iron-rich" delusion by incorporating Pt. In vitro tests demonstrate that deferoxamine (DFO), an iron depletion drug exhibits an iron-depletion effect on human intestinal Caco-2 cells, but not on HepG2 cells (Fig. 2A). Our bioinorganic ferroxidase depleted iron in both types of cells (Fig. S6). Furthermore, the ferritin

composites did not inhibit the cellular iron uptake in the way DFO does when an excess of iron is supplemented (Fig. S7). In such circumstances, apoferritin apparently acts as an iron sponge and container for intracellular storage.

Also in presence of Zn^{2+} that competitively inhibits also the cellular iron uptake,[12] the composites with ferroxidase activity stabilize the intracellular iron level (Fig. 2B). It seems that the ferroxidase activity of apoferritin plays a role in the cellular response to Zn^{2+}-induced inhibition. The significant difference between the ferroxidase active Pt-huFL and inactive apo-huFL indicates that the encapsulated ferroxidase-mimetic Pt nanoparticles facilitate the stabilizing effect of Pt-huFL on the intracellular iron. This observation verifies the resistance of Pt-containing ferritin to the Zn^{2+}-induced inhibition also in a cellular environment.

The changes of the cellular iron uptake through the transferrin receptor (TfR) and its export through ferroportin have direct effects on the cellular iron.[13,14] To address the mechanism of iron-regulation effects of Pt-huFL , the translational changes of TfR and ferroportin on Caco-2 and HepG2 cells were investigated upon the treatments. No effects of DFO on both iron transporters were observed from Caco-2 and HepG2 cells (Fig. 2C). In contrast, Pt-huFL and apo-huFL increased the membrane level of TfR on Caco-2 cells. An obvious increase of ferroportin upon treatment with Pt-huFL was observed on HepG2 cells. In contrast to the sole iron-depleting function of DFO, the ferritin-based composites influence the cellular iron apparently in a more biological and physiological way. Most important is the apoferritin confines the bioactivity of the Pt nanoparticles in an iron specific manner.

In conclusion, Pt nanoparticles as the enzyme active site enhance the ferroxidase activity, stability and the mineralization ability of apoferritin. The designed inhibitor-resistant bioinorganic ferroxidase influences the cellular iron homeostasis. The hybrid nature of the engineered enzyme enables its cellular iron regulation in a physiologically favorable way, making favorable use of both the inorganic and bio-organic constituents. The demonstrated possibility to use inorganic nanomaterials to fabricate artificial enzymes shows new insights with great promise for enzyme design for future biomedical applications.

M.K. and U.C. greatly acknowledge financial support through Marie Curie Actions (CIG) within project number 322158 (ARTEN). The authors greatly acknowledge financial support by the Spanish ministry of economy and competitivity (MINECO) through project number MAT2012-38161 and the Basque government through project number PI2013-56.

Notes and references

[a] CIC nanoGUNE, Tolosa Hiribidea 76, 20018 Donostia-San Sebastian, Spain. E-mail: l.zhang@nanogune.eu; m.knez@nanogune.eu.

[b] IKERBASQUE, Basque Foundation for Science, Alameda Urquijo 36-51, 48011 Bilbao, Spain.

† Electronic Supplementary Information (ESI) available: details of materials and methods. Supporting figure S1-S7. See DOI: 10.1039/c000000x/

1 G. Vriend, *Science* **2004**, *306*, 1135.
2 H. Wei, E. Wang, *Chem. Soc. Rev.* **2013**, *42*, 6060-6093.
3 a) J. G. Lieghr, J. S. Jones, Curr. Med. Chem. 2001, 8, 839. b) S. Cherukuri, R. Potla, J. Sarkar, S. Nurko, Z. L. Harris, P. L. Fox, *Cell Metab.* **2005**, *2*, 309. c) J. M. Fernandez-Real, A. Lopez-Bermejo, W. Ricart, *Diabetes* **2002**, *51*, 2348.
4 S. Olivieri, A. Conti, S. Iannaccone, C. V. Cannistraci, A. Campanella, M. Barbariga, F. Codazzi, I. Pelizzoni, G. Magnani, M. Pesca, D. Franciotta, S. F. Cappa, M. Alessio, *J. Neurosci.* **2011**, *31*, 18568.
5 J. A. Duce, A.Tsatsanis, M. A. Cater, S. A. James, E. Robb, K. Wikhe, S. L. Leong, K. Perez, T. Johanssen, M. A. Greenough, H. H. Cho, D. Galatis, R. D. Moir, C. L. Masters, C. McLean, R. E. Tanzi, R. Cappai, K. J. Barnham, G. D. Ciccotosto, J. T. Rogers, A. I. Bush, *Cell* **2010**, *142*, 857.
6 E. C. Theil, R. K. Behera, T. Tosha, *Coord. Chem. Rev.* **2013**, *257*, 579.
7 a) T. Douglas, D. P. Dickson, S. Betteridge, J. Charnock, C. D. Garner, S. Mann, *Science* **1995**, *269*, 54. b) X. Liu, W. Wei, Q. Yuan, X. Zhang, N. Li, Y. Du, G. Ma, C. Yan, D. Ma, *Chem. Comm.* **2012**, *48*, 3155. c) A. Sennuga, J. van Marwijk, C. Whiteley, *Nanomed. Nanotech. Biol. Med.* **2013**, 9, 185–193. d) U. Carmona, L. Zhang, L. Li, W. Münchgesang, E. Pippel, M. Knez, *Chem. Commun.* **2014**, *50*, 701.
8 a) L. Zhang, L. Laug, W. Münchgesang, E. Pippel, U. Gösele, M. Brandsch, M. Knez, *Nano Lett.* **2010**, *10*, 219. b) J. Fan, J. Yin, B. Ning, X. Wu, Y. Hu, M. Ferrari, G. J. Anderson, J. Wei, Y. Zhao, G. Nie, *Biomaterials* **2011**, *32*, 1611. c) L. Zhang, W. Fisher, E. Pippel, M. Brandsch, M. Knez, *Small*, **2011**, *7*, 1538.
9 a) F. Bou-Abdallah, G. Biasiotto, P. Arosio, N. D. Chasteen, *Biochemistry* **2004**, *43*, 4332. b) S. Pfaffen, R. Abdulqadir, N. E. Le Brun, M. E. P. Murphy, *J. Biol. Chem.* **2013**, *288*, 14917.
10 a) M. A. Baraibar, A. G. Barbeito, B. B. Muhoberac, R. Vidal, *Free Radic. Biol. Med.* **2012**, *52*, 1692–1697. b) G. Zhao, F. Bou-Abdallah, X. Yang, P. Arosio, N. D. Chasteen, *Biochemistry* **2001**, *40*, 10832.
11 a) Y. Tsuji, H. Ayaki, S. P. Whitman, C. S. Morrow, S. V. Torti, F. M. Torti, *Mol. Cell. Biol.* **2000**, *20*, 5818-5827. b) E. C. Pietsch, J. Y. Chan, F. M. Torti, S. V. Torti, *J. Biol. Chem.* **2003**, *278*, 2361.
12 J. Tallkvist, C. L. Bowlus, B. Lönnerdal, *Am. J. Clin. Nutr.* **2000**, *72*, 770.
13 M. F. Macedo, M. de Sousa, *Inflamm. Allergy Drug Targets* **2008**, *7*, 41.
14 A. Donovan, C. A. Lima, J. L. Pinkus, G. S. Pinkus, L. I. Zon, S. Robine, N. C. Andrews, *Cell Metab.* **2005**, *1*, 191.